PHYTOTHERAPY RESEARCH
Phytother. Res. **20**, 970–980 (2006)
Published online 16 August 2006 in Wiley InterScience
(www.interscience.wiley.com) **DOI**: 10.1002/ptr.1991

Tumor Cell Specific Toxicity of *Inula helenium* Extracts

David C. Dorn[1], Maja Alexenizer[2], Jan G. Hengstler[3] and August Dorn[2,*]

[1]Laboratory of Developmental Hematopoiesis, Cell Biology Program, Memorial Sloan-Kettering Cancer Center, 1275 York Avenue, New York, NY 10021, USA
[2]Institute of Zoology, Johannes Gutenberg University, D-55099 Mainz, Germany
[3]Center for Toxicology, Institute for Legal Medicine and Rudolf Boehm-Institute for Pharmacology and Toxicology, Haertelstr. 16-18, D-04347 Leipzig, Germany

The aim of the research program was to identify botanical extracts with antineoplastic activity. In this respect extracts prepared from *Inula helenium* roots showed a remarkable activity. As evidenced by the MTT assay, the *Inula helenium* extract revealed a highly selective toxicity toward four different tumor cell lines (HT-29, MCF-7, Capan-2 and G1), but a much lower toxicity against healthy human peripheral blood lymphocytes (PBLs) from two donors. The extract-induced death of tumor cells was studied extensively by electron microscopy. There was a remarkable similarity of morphological alterations observed in the four cell lines: patchy chromatin condensations, cytoplasmic vesiculation, swelling and rupture of mitochondria. The morphology of cellular breakdown bore more resemblance to necrotic than to apoptotic cell death, which was supported by the failure to mark early apoptotic events by Annexin V. It has been pointed out recently that compounds inducing cell death with necrotic-like morphology could be very beneficial in cases where cancerous cells have gained resistance to apoptosis. In this context, the remarkable difference in cytotoxicity exerted by the *Inula helenium* extract, which was over 100-times higher in the tumor cell lines than in the PBLs, makes the extract an excellent candidate for further anticancerous investigations, especially since the *Inula helenium* extract was not mutagenic in the Ames test.

Keywords: plant extract; *Inula helenium*; anticancerous activity; necrotic-like cell death; low toxicity against PBL.

INTRODUCTION

In recognition of nature's potential – and the need to replace drugs that have become ineffective by emerging resistance – several large-scale plant screenings were performed in the 1960s and 1970s. During this time, The American Cancer Institute (NCI) sponsored an extensive program screening about 35 000 plant species for anticancer activity which led to the discovery of taxol (paclitaxel) from the Pacific Yew tree, *Taxus brecifoli*. Later, another anticancer agent, docetaxel, was isolated from the European Yew, *Taxus baccata*. Today, the taxanes are one of the most powerful classes of compounds among all chemotherapeutic drugs, exhibiting a wide range of activity and are of special benefit in fighting metastatic breast, ovarian and lung cancer (Crown *et al.*, 2004; Gligorov and Lotz, 2004). Other natural compounds, in particular the vinca alkaloids from the periwinkle plant, *Vinca rosea*, are well known cytostatics (Van Tellingen *et al.*, 1992). The introduction of high-throughput synthesis and combinatorial chemistry in recent years has led to a decline in the screening of natural products by the pharmaceutical industry, which is now considered as a premature decision (Ortholand and Ganesan, 2004). In a call for 'back to the future' the advantage of using 'crude' botanical extracts has been emphasized as opposed to the standard approach which has been to isolate, synthesize and administer the single chemical compound thought to be responsible for the effect of the extract (Vickers, 2002). The different components in a botanical may have synergistic activities and the presence of multiple compounds in an extract can buffer the toxic effects of a single constituent (Vickers, 2002). The present study aimed to discover such a botanical extract, which we believe has been obtained by the extract of *Inula helenium*.

Inula helenium is a well-known medicinal plant. Originally native to Southeast Europe, it has been introduced to Central Europe, the Near East, many other parts of Asia, and to the Northeast of the USA. Preparations of its roots are used in the folk medicine of several ethnics against a variety of ailments including asthma, (whooping) cough, bronchitis, lung disorders, tuberculosis, indigestion, chronic enterogastritis, infectious and helminthic diseases (List and Hörhammer, 1976; Cantrell *et al.*, 1999; Dachler and Pelzmann, 1999; Konishi *et al.*, 2002). Recently, antiproliferative activity of root extracts from *I. helenium* was reported in two human and a murine neoplastic cell line (Konishi *et al.*, 2002). This is a study, in greater detail, of the effects of an extract of *I. helenium* on four human carcinoma cell lines in comparison with healthy peripheral blood lymphocytes (PBLs). The extract exerted a strong

* Correspondence to: August Dorn, Institute of Zoology, Johannes Gutenberg University, D-55099 Mainz, Germany.
E-mail: dorn@uni-mainz.de

Received 25 October 2005
Accepted 20 July 2006

antiproliferative, necrotic-like effect on the carcinoma cells but a much lesser cytotoxic effect on healthy PBLs.

MATERIALS AND METHODS

Extracts of *Inula helenium*. For the extraction procedure, dried roots were ground into a powder and 30 g of the powder was incubated with 100 mL of the solvent, acetone:methanol = 2:1 (v/v). Acetone (≥99.5%) and methanol (≥99.8%) were from Roth, Karlsruhe, Germany. The extraction was carried out over 7 days at room temperature (22 ± 2 °C). The extraction suspension was shaken daily for 10 min. After 7 days, the suspension was filtered, the filtrate representing the 'standard concentration'. The extract was stored in capped dark glass bottles at room temperature and tested within a month after preparation.

Tumor cell lines. The human tumor cell lines HT-29 (colon cancer), MCF-7 (breast cancer), Capan-2 (pancreatic cancer) and G1 (astrocytoma) were kindly provided by Dr Gabriele Pecher (Department of Internal Medicine, Medical Oncology and Hematology, Humboldt-University Berlin, Charité Campus Mitte, 10115 Berlin, Germany). All human cell lines were grown in Dulbecco's modified Eagle medium (DMEM) (Gibco BRL, Eggenstein, Germany) supplemented with 10% inactivated fetal calf serum (FCS) (Biochrom, Berlin, Germany) and 10 μg/mL gentamycin sulphate (Sigma, Deisenhofen, Germany) in a humidified atmosphere of 5% CO_2–95% air at 37 °C.

Blood cells. Peripheral blood mononuclear cells (PBMC) were isolated from heparinized peripheral blood of healthy donors. After density centrifugation over a Lymphoprep-Plaque (1.077 g/mL; Nycomed, Unterschleissheim, Germany) cells were removed from the interphase and resuspended in RPMI-1640 (Gibco BRL, Eggenstein, Germany). The lymphocytes were enriched by removing the thrombocytes in four consecutive centrifugations (1000 rpm, 10 min, 4 °C) each time resuspending the pellet with 14 mL of RPMI-1640.

Cytotoxicity. Cellular viability in the presence or absence of experimental agents was determined using the microculture tetrazolium assay MTT (3-[4,5-dimethylthiazol-2-yl]-2,5-diphenyltetrazolium bromide) (Sigma, Deisenhofen, Germany). A 96-well plate (Nunc, Wiesbaden, Germany) was prepared and 10, 1, 0.1, 0.05, 0.01 and 0.005 μL of the extract were placed in the individual wells. As negative controls the solvent and untreated cells were included; as positive controls no cells were seeded simulating a 100% cell death. Prior to seeding the cells, the solvent and the extract were evaporated onto the bottom of the wells. Next, the wells were refilled with 200 μL of tissue culture medium (as described above) per well. Then tumor cell suspensions were obtained by trypsination of the monolayer cultures (using trypsin from BioWhittaker Europe, Taufkirchen, Germany) and were plated in a concentration of 2×10^4 cells per well. After a 24 h incubation period all non-adherent cells in the wells were removed by performing four consecutive washes with PBS supplemented with 2% FCS using a multipipette. After washing 50 μL of MTT in a solution of 2 mg/mL was added to each well together with 150 μL of tissue culture medium. Subsequently the cells were incubated for 4 h at 37 °C. After that the supernatant of the wells was removed and the formazan crystals formed in the viable cells were dissolved by adding 150 μL of dimethyl sulfoxide (DMSO) (Sigma). The optical density (OD) was read at a wavelength of 550 nm using a microplate reader. The viability was calculated as OD with drug/OD without drug. Each experiment was repeated twice and prepared as triplicate wells.

Flow cytometry. For the FACS analysis the ApoAlert Annexin V-FITC Kit (BD Bioscience) was used to detect apoptosis. The cells were plated in 6-well plates (Nunc) in a concentration of 2×10^5/well in which the extract was previously evaporated onto the well bottom in a concentration of 10-times the LD_{50}: HT-29 = 0.15 μL/mL; MCF-7 = 0.17 μL/mL; Capan-2 = 0.2 μL/mL; G1 = 0.18 μL/mL. After 6 h of incubation the treated cells were detached through trypsination and prepared for FACS analysis. As negative controls solvent treated cells were included. The cells were washed with ice cold PBS and resuspended in 100 μL binding buffer (1×10^6/mL) adding 5 μL of Annexin V-FITC and 5 μL PI. After 15 min of incubation at 25 °C in the dark, the cells were diluted with 400 μL of binding buffer and immediately analysed. All FACS analyses were performed as triplicates and repeated twice.

Electron microscopy. Prior to fixation, adherent cells were harvested with trypsin (0.05%), washed with PBS and transferred into centrifugation tubes. The cells were then gently centrifuged (600 rpm), and the supernatant was removed. The cell pellet was resuspended in fixative: 2.5% glutaraldehyde in 0.08 M cacodylate buffer (pH 7.4) with 0.1 M sucrose. After 1 h, the suspension was centrifuged (600 rpm), the pellet was washed in cacodylate buffer (3 × 20 min) and was placed in 2% osmium tetroxide for 1 h. Then, the pellet was washed in distilled water, dehydrated via increasing concentrations of ethanol and embedded in araldite. Sections of about 70 nm thickness were double-stained in uranyl acetate and lead citrate. Transmission electron microscope studies were performed with a Zeiss EM900.

Ames test. The mutagenicity experiments with his^- *S. typhimurium* were performed with minor modifications of the method described by Ames *et al.* (1975). Mutagenicity was studied with *Salmonella typhimurium* TA 1535, TA 100, TA 1537, TA 98 and TA 102. The *Inula helenium* extract was tested in the presence and absence of rat liver S-9 Mix as an activating system. The experiments were conducted as a preincubation assay. The extract of *Inula helenium* was dissolved in DMSO immediately before use. In this study solvent (DMSO) treated cultures were used as negative controls. To confirm the sensitivity of the bacterial strains against mutagens and to ensure the activity of the exogenous metabolizing system several positive controls were included. An exogenous metabolizing system 2-aminoanthracene (10.0 μg per plate A3,880-0, batch 0013406) and benzo[α]pyrene (10.0 μg per plate; Sigma B-1760, batch 11OH0096) were used for all strains. Without metabolic activation the following compounds were used as positive controls: For the

DOI: 10.1002/ptr

strains TA 1535, TA 100, TA 1537 and TA 98 benzo[α]pyrene 4,5-oxide (0.25 µg per plate; synthesis according to Harvey *et al.*, 1975) and *N*-methyl-*N*′-nitro-*N*-nitrosoguanidine (0.25 µg per plate) were tested. Cumene hydroperoxide (25 µg per plate) was used with TA 102.

To estimate toxicity, his$^+$ bacteria were added as an internal standard to otherwise normal mutagenicity plates. The his$^+$ bacteria used are spontaneous revertants from TA 1537. They were added to plates together with a strain which gives low numbers of revertant colonies (TA 1537). The difference in the number of colonies on the plates with and without added his$^+$ bacteria, in the presence of test compound, was compared with the value obtained with solvent controls. The ratio of these two values gives the surviving fraction.

RESULTS

Cytotoxicity of the extract

The cytotoxicity of the *Inula helenium* extract was measured by the MTT assay for adherent cell lines and propidium iodide staining and FACS analysis for PBL. There was hardly any variability in the sensitivity of the four different tumor entities towards the extract as demonstrated in Fig. 1A–D. The extract showed a concentration-dependent cytotoxic effect on all tested human carcinoma cell lines (HT-29, MCF-7, Capan-2, and G1) with a LD_{50} at concentrations (µL 'standard extract'/mL medium) of 0.015 for HT-29, of 0.017 for MCF-7, of 0.020 for Capan-2 and of 0.018 for G1 and a LD_{90} at concentrations of 0.05 for HT-29, of 0.20 for MCF-7, of 0.10 for Capan-2 and of 0.10 for G1 (Table 1). The cytotoxicity measurements on the healthy human PBLs from two separate donors resulted in a significantly higher tolerability of the extract (Fig. 1E) with a LD_{50} of 2.4 and of 3.0, respectively, and a LD_{90} of 8.0 and of 9.0, respectively (Table 1). Thus, the LD_{50} of healthy PBLs exceeded the LD_{50} of the carcinoma cells by more than 120-fold (donor 1) and by more than 150-fold (donor 2), respectively.

Examination of the extract-induced cell death by the early apoptosis marker Annexin V

No significant apoptotic events could be demonstrated with the early apoptosis marker Annexin V 6 h after treatment (Fig. 2). Twenty four hours after treatment, over 90% of the cells stained with propidium iodide indicating cell death by necrosis with no major increased

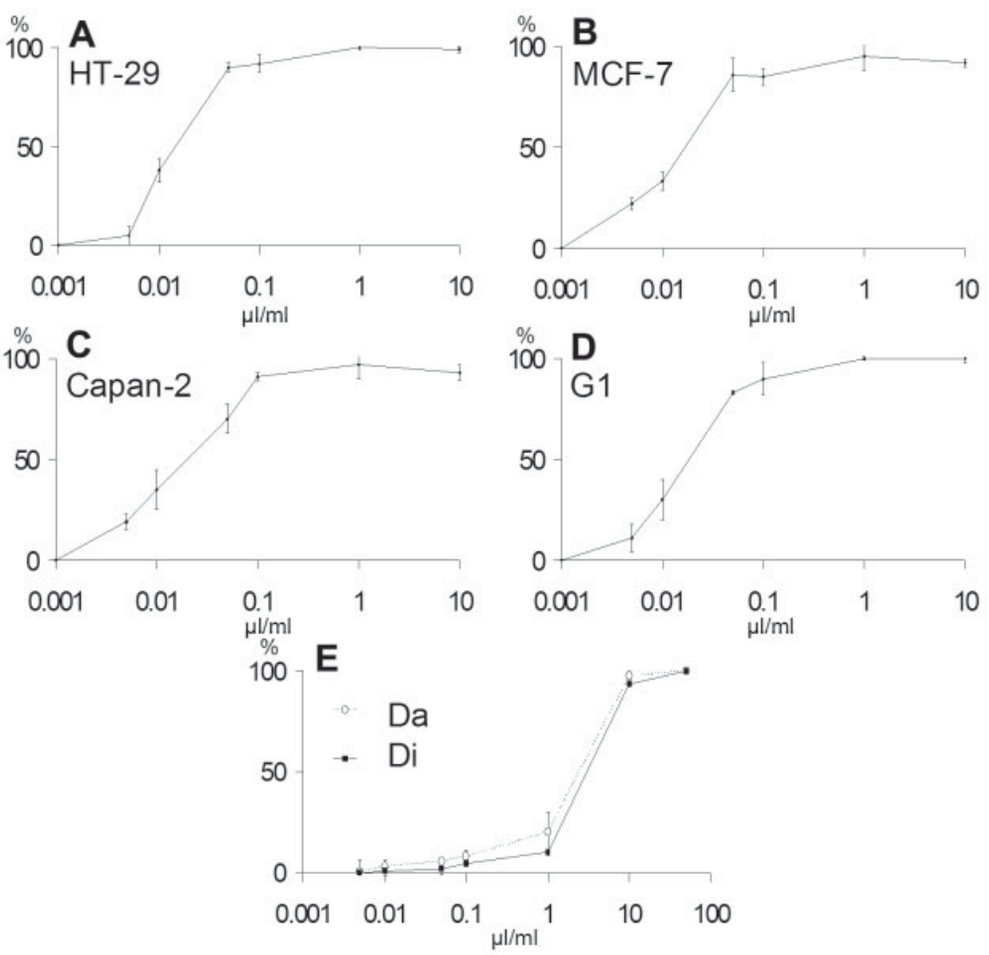

Figure 1. Toxicity of *Inula helenium* extract to four different tumor cell lines (A–D: HT-29, MCF-7, Capan-2 and G1) as well as to healthy PBL of two donors (E). Analysis was performed by the MTT test, whereby 0% corresponds to the controls and 100% to complete cell death. Graphs are mean values of at least three experiments. Bars indicate standard deviations.

DOI: 10.1002/ptr

Table 1. Cytotoxicity (LD_{50} and LD_{90}) of the *Inula helenium* extract. Concentrations are given in µL 'standard extract'/mL culture medium

Cells	HT-29	MCF-7	Capan-2	G1	PBL Da	PBL Di
LD_{50}	0.015	0.017	0.020	0.018	2.4	3.0
LD_{90}	0.05	0.20	0.10	0.10	8.0	9.0

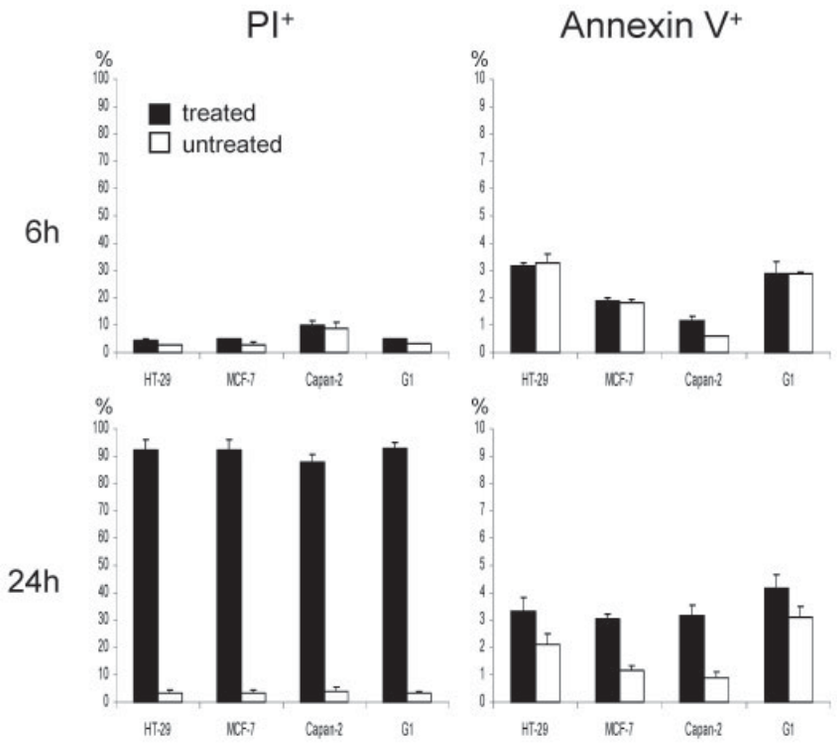

Figure 2. Annexin-V staining for early apoptosis. The cells were treated with *Inula helenium* extract in the 10-fold concentration of LD_{50}. The percentage of PI^+ single and double stained cells (PI^+) after 6 h and 24 h is given (left graphs). Right graphs depict the percentage of Annexin-V single positive stained cells, resembling the apoptotic fraction. Mean values are given with standard error bars of two triplicate experiments.

Annexin V single stained apoptotic fraction. To further elucidate the character of cell death electron microscope studies were carried out to define subcellular morphological events.

Electron microscope analysis of cell death induced by *I. helenium* extract

HT-29. The human colon carcinoma cell line HT-29 shows epithelial growth under normal and control conditions (see Materials and Methods), and also the ultrastructural features do not differ between cells kept in standard medium and those incubated with the addition of the solvent of the extract. The nuclei of these cells have a somewhat irregular shape and include exceptionally large nucleoli; the chromatin is rather evenly distributed (Fig. 3a). The most outstanding cell organelles are the extraordinary large mitochondria with tightly packed cristae embedded in a rather electron-dense matrix which includes electron-lucent areas ('vacuoles') spared by cristae, and with dark granules (Fig. 3b). The cytoplasm contains many free ribosomes, primary and secondary lysosomes, few clear, non-membrane-bound vesicles and intermediate filaments (Fig. 3a, b). Endoplasmic reticulum (ER) and Golgi complexes are rare, but coated vesicles abundant.

HT-29 cells incubated with the extract, detach from the bottom of the culture flask, round up and become solitary. At first, the nuclei of treated cells show a slight patchy aggregation of chromatin, mostly at the nuclear envelope, the double membrane of which is often somewhat distended and the space in between electron-lucent (Fig. 3c). At higher concentrations of the extract chromatin clumping becomes more intense. Most conspicuous is the vesiculation of the cytoplasm which increases with time and higher concentration of the extract (Fig. 3c). The vesicles have irregular profiles, are electron-lucent and non-membrane-bound. The mitochondria become smaller after treatment – probably by fragmentation – but the packing of the cristae is less compact, the matrix less electron-dense, and the 'vacuoles' are larger than in mitochondria of normal and control cells (Fig. 3c, d). Although the mitochondria are now smaller, they appear swollen and their membranes have occasionally ruptured (Fig. 3d). Secondary lysosomes increase after treatment. Intermediate filaments are condensed and often form a ring around the nucleus (Fig. 3c). Other organelles (e.g. Golgi

DOI: 10.1002/ptr

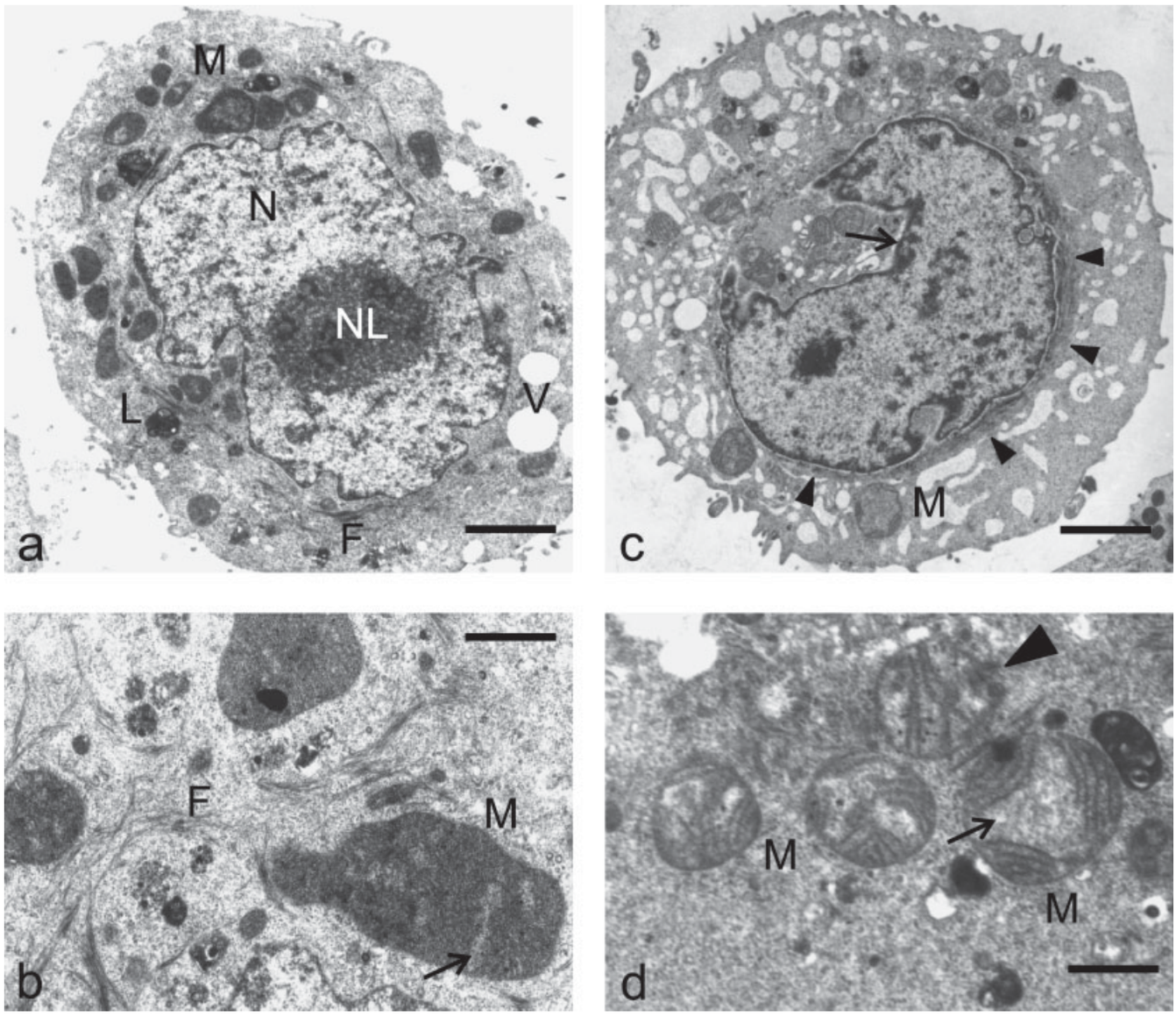

Figure 3. Electron micrographs. HT-29 cells: non-treated (a, b) and treated (c, d). (a) The nucleus (V) of this normal cell contains rather evenly distributed chromatin and a large nucleolus (NL). Mitochondria (M) are extraordinary large. F, intermediate filaments; L, lysosome; V, electron-lucent vesicle. Bar = 1.87 μm. (b) Mitochondria (M) of normal cell at higher magnification. Arrow points to electron-lucent area, 'vacuole', in mitochondrial matrix. F, intermediate filaments. Bar = 0.90 μm. (c) Cell treated with extract (1 μL/mL). The chromatin forms patchy aggregations, primarily at the nuclear envelope. The nuclear double membrane is slightly distended and shows an electron-lucent interspace (arrow). The cytoplasm is strongly vacuolized. Arrow heads point to a ring of intermediate filaments around the nucleus. M, mitochondrion. Bar = 2.83 μm. (d) Mitochondria (M) of treated cell (0.1 μL/mL): they appear swollen and the 'vacuoles' have expanded (arrow). Arrow head indicates rupture of the mitochondrial membrane. Bar = 0.94 μm.

complexes, ER and concentration of free ribosomes) experience no discernible changes.

MCF-7. The human mamma carcinoma cell line MCF-7, like HT-29, shows epithelial-like growth, and the cells are attached to the bottom of the culture flask under normal and control conditions. Nuclear profiles are very irregular, the chromatin is evenly distributed, and nucleoli are voluminous (Fig. 4a). The cytoplasm includes many free ribosomes, few cisternae of rough ER, inconspicuous Golgi complexes but many lysosomes. The mitochondria, of the crista type, are of average size, and their matrices of medium electron density (Fig. 4b). Lipid droplets are observed in various numbers, strands of intermediate filaments are scattered throughout the cytoplasm (Fig. 4a). The large amount of coated vesicles indicates a high rate of metabolism.

Treated cells detach, give up their epithelial-like organization and float singularly. The most pronounced changes after treatment concern a vacuolization of cytoplasm depending on the concentration of the extract. The vacuoles, at first small with irregular contours (Fig. 4c), become bigger and rounded (Fig. 4d). They are always non-membrane-bound, and not identical with the lipid droplets which are seen in non-treated cells (Fig. 4c). Another important change is the swelling of mitochondria. Their cristae become disorganized, the matrix expands, and the mitochondrial membrane eventually ruptures (Fig. 4e, f). The intermediate filaments tend to condense and enwrap cellular compartments,

DOI: 10.1002/ptr

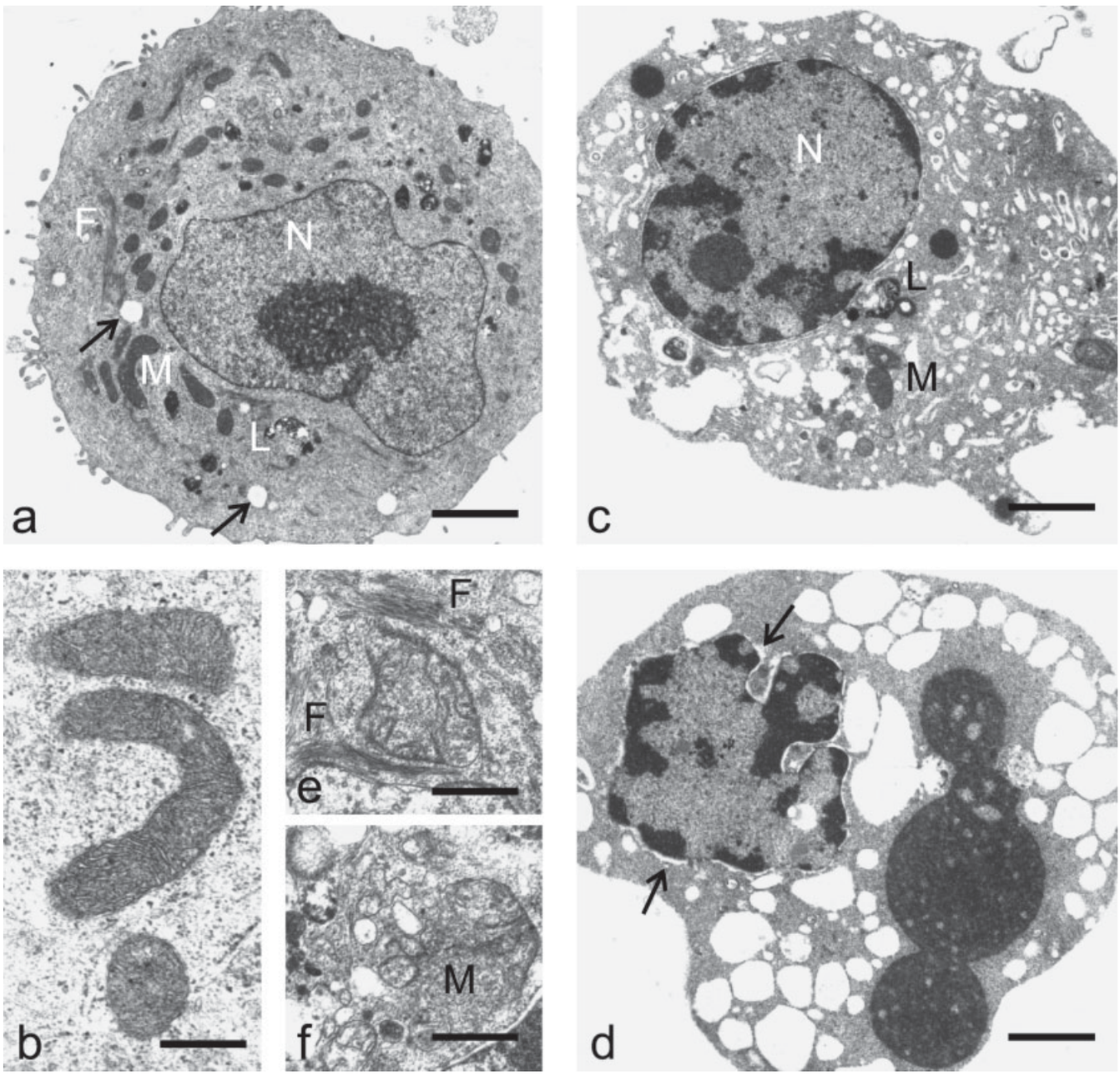

Figure 4. Electron micrographs. MCF-7 cells: non-treated (a, b) and treated (c–f). (a) Nucleus (N) of normal cell with evenly distributed chromatin and large nucleolus. F, intermediate filaments; L, lysosomes; M, mitochondria; arrows point to lipid droplets. Bar = 2.76 μm. (b) Mitochondria of normal cell. Bar = 0.50 μm. (c) Treated cell (1 μL/mL). Patchy chromatin condensations are mostly located at the envelope of the nucleus (N). The cytoplasm is interspersed with many small electron-lucent vesicles of irregular profile. M, mitochondria; L, lysosomes. Bar = 1.75 μm. (d) Progressed vesiculation and chromatin condensation of treated cell (1 μL/mL). Arrows point to distended nuclear envelope with electron-lucent interspace. Note remnant of phagocytized cell. Bar = 1.81 μm. (e) Swollen and disorganized mitochondrion surrounded by intermediate filaments (F) in treated cell (1 μL/mL). Bar = 0.75 μm. (f) Damaged and ruptured mitochondrion (M) in treated cell (1 μL/mL). Bar = 0.75 μm.

like defective mitochondria (Fig. 4e), aggregations of secondary lysosomes, or the nucleus. Similar to treated HT-29 cells, chromatin aggregates in patches at the nuclear envelope which slightly distends and appears as an electron-lucent nuclear lining (Fig. 4c, d). Cells have been observed to phagocytize each other (Fig. 4d).

Capan-2. Under normal and control conditions, the human pancreas carcinoma cell line, Capan-2, grows as a monolayer of polygonal cells and expresses epithelial-like features. The nuclei are slightly irregular in shape, the nucleoli very big, the chromatin is rather evenly dispersed (Fig. 5a, b). The cytoplasm contains many free ribosomes, scattered cisternae of rough ER with moderately electron-dense content, and well expressed Golgi complexes. The mitochondria are relatively small, their cristae often slightly distended, the matrix is electron-dense (Fig. 5a, b). The cells include various numbers of lysosomal bodies (Fig. 5a) and randomly distributed bundles of filaments (Fig. 5c). Coated vesicles are frequently observed.

DOI: 10.1002/ptr

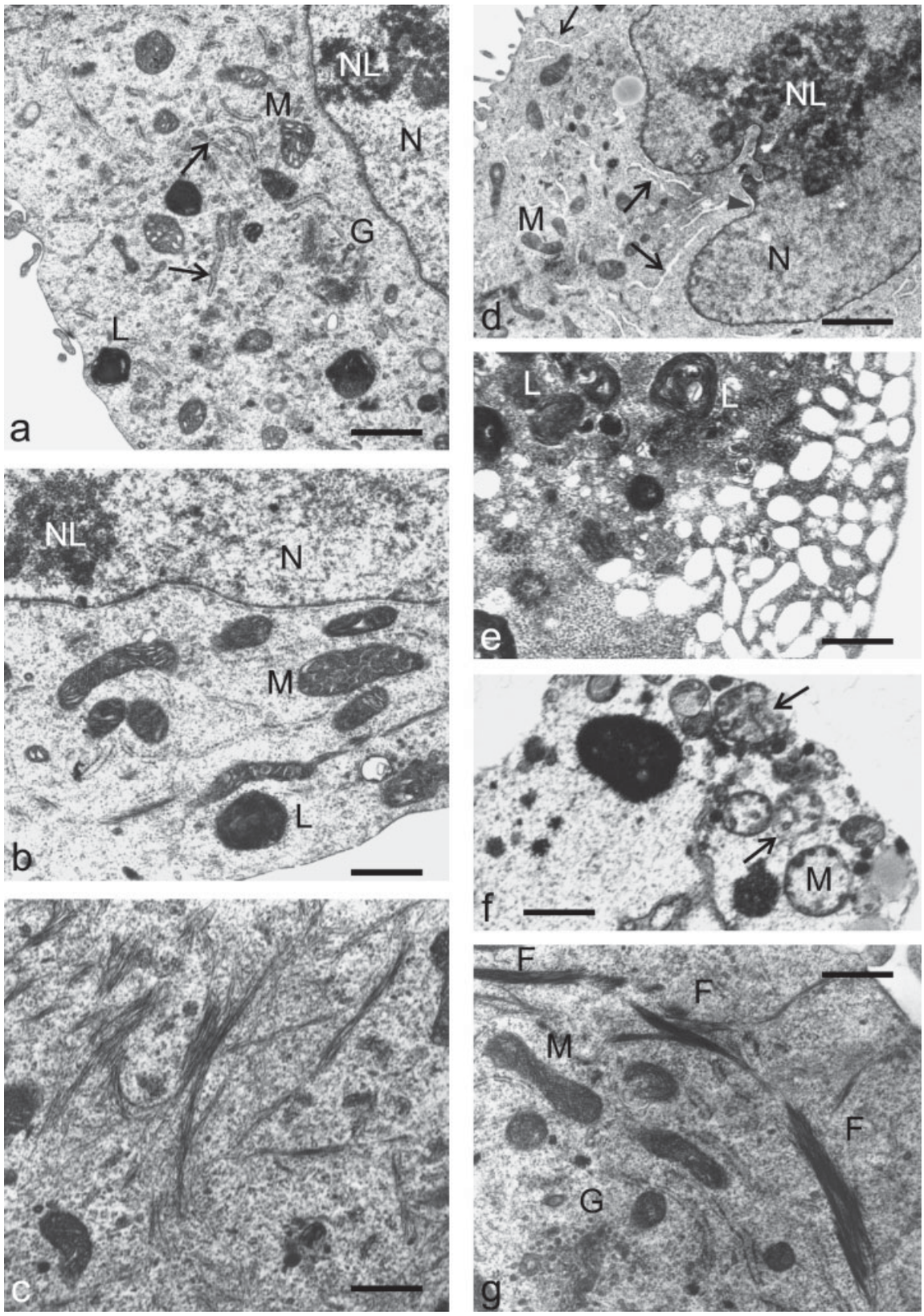

Figure 5. Electron micrographs. Capan-2 cells: non-treated (a–c) and treated (d–g). (a) Normal cell displaying short strands of RER (arrows), Golgi complex (G), mitochondria (M) and lysosomes (L). N, nucleus; NL, nucleolus. Bar = 1.02 μm. (b) Normal cell with nucleus (N) showing evenly distributed chromatin; mitochondria (M) have a rather electron-dense matrix. L, lysosome; NL, nucleolus. Bar = 0.67 μm. (c) Normal cell with randomly scattered bundles of intermediate filaments. Bar = 0.67 μm. (d) Treated cell (0.1 μL/mL). Early reactions to the extract: slight distension of the RER (arrows) and the nuclear envelope (arrow head) with electron-light interspace. N, nucleus; NL, nucleolus. Bar = 2.37 μm. (e) Treated cell (0.1 μL/mL). Late effects caused by the extract: strong vesiculation of the cytoplasm and increase of lysosomal bodies (L). Bar = 0.61 μm. (f) Swollen mitochondria (M), partly ruptured (arrows), in treated cell (0.1 μL/mL). Note large lysosomal body. Bar = 0.80 μm. (g) Treated cell (0.1 μL/mL). Bundles of intermediate filaments (F) appear condensed, compared with non-treated cells (see Fig. 5c) and arranged in a ring. G, Golgi complex; M, mitochondrion. Bar = 0.72 μm.

DOI: 10.1002/ptr

Treated Capan-2 cells detach, give up epithelial-like organization and round up. A high concentration of the extract provokes the formation of small clumps of chromatin (not shown). The lower concentration causes, at first, a slight distension of the cisternae of the rough ER, the content of which is now electron-lucent (Fig. 5d). Then, vesiculation of the cytoplasm takes place and complex lysosomal bodies become more numerous (Fig. 5e). Mitochondria become swollen, disorganized and finally rupture (Fig. 5f). Intermediate filaments condense and show a higher degree of organization than in non-treated cells (Fig. 5c, g). Other cell organelles – Golgi complexes, abundance of free ribosomes and coated vesicles – appear unchanged (Fig. 5g) until the disintegration of the cells.

G1. The G1 cell line originates from a second grade human astrocytoma and grows epithelial-like. The large nuclei of the cells are bizarre and deeply lobed. Nucleoli are not conspicuous, the chromatin is organized in randomly scattered flakes (Fig. 6a). Besides many free ribosomes, the cytoplasm includes many singular strands of rough ER which are sometimes considerably distended and harbour fine granular material of moderate electron density (Fig. 6a). The relatively small mitochondria are of the crista type and have an electron-dense matrix (Fig. 6a, b). Golgi complexes are surrounded, especially at their inner, concave parts, by an accumulation of many small vesicles creating an extended Golgi zone (Fig. 6b). The cells contain few lysosomal bodies and very few electron-lucent vesicles. Coated vesicles are much less frequent than in the other cell lines used in this study. Most intriguing, however, are tubular structures occurring in the non-treated G1 cells. They may be enclosed in lysosome-like and lamellar, myelin-like, bodies or be located singularly or in small groups in condensations of the cytoplasmic matrix (Fig. 6c and Inset). The longest tubules measured 910 nm, the diameter varied between 61.4 nm and 216 nm. The walls of the tubules consist of one to three electron-dense laminae (Fig. 6c Inset). The nature of the tubules is unknown.

After treatment, the cells detach, become solitary and round off. The nucleus often adopts a cup-shaped appearance embracing a Golgi zone and mitochondria (Fig. 6d). The chromatin flakes condense (Fig. 6d, e). Round vesicles of various sizes appear in the cytoplasm. They are electron-lucent, but contain a fine fibrous material (Fig. 6e). The vesicles can become very large by fusion. Mitochondria change in appearance: the matrix becomes less electron-dense and the cristae are not as tightly packed as in non-treated cells (Fig. 6f). The tubular inclusions are not affected by the treatment.

Mutagenicity of *I. helenium* extract

The extract of *I. helenium* was tested for mutagenicity with and without the addition of rat liver S-9 Mix as a metabolizing system. Concentrations of 0.31, 1.00, 3.16, 10.0 and 31.6 μg per plate were used. Higher concentrations could not be tested since *I. helenium* was toxic to *Salmonella typhimurium*. *I. helenium* did not show any mutagenicity in the Ames test with or without the addition of S-9 Mix as an exogenous metabolizing system. A representative example of the data obtained in an Ames test with S-9 Mix is shown in Table 2. A strong increase in the number of revertants was obtained for the positive control substance 2-aminoanthracene for tester strains TA 98, TA 100, TA 102 and TA 1535, whereas benzo[α]pyrene increased the number of revertants for TA 98, TA 100, TA 102 and TA 1537, indicating a good sensitivity of the bacterial strains and functioning of the metabolizing system (Table 2). In conclusion, extracts of *I. helenium* used in the present study were not mutagenic in *S. typhimurium* but were toxic to the bacteria at 10 and 31.6 μg/plate.

DISCUSSION

The extract of *I. helenium* was cytotoxic to four cancer cell lines. Interestingly, cytotoxicity in cancer cells was observed at more than 100-fold lower concentrations compared with healthy human peripheral blood lymphocytes. Furthermore, the extract of *I. helenium* was not mutagenic in the Ames test with and without rat liver S-9 Mix as an exogenous metabolizing system. Thus, the *I. helenium* extract used in this study caused a tumor cell specific toxicity without being mutagenic.

The course of cell death was elucidated by physiological and morphological parameters. Annexin V was

Table 2. Mutagenicity experiments with his$^-$ *S. typhimurium* were performed as described by Ames *et al.* (1975) with minimal modifications. This table shows the mean numbers of revertant colonies of three plates and standard deviations. To estimate toxicity, his$^+$ bacteria (RTA) that are spontaneous revertants of TA 1537 were used. Relative survival gives a measure for toxicity of the test substance to RTA and was calculated as described in Materials and Methods

	Salmonella typhimurium test strain						
Inula helenium extract (μg/plate)	TA 98	TA 100	TA 102	TA 1535	TA 1537	RTA	Relative survival
0.00	11 ± 5	72 ± 7	84 ± 7	10 ± 3	9 ± 3	100 ± 13	1.00
0.31	9 ± 3	82 ± 7	78 ± 12	16 ± 2	7 ± 1	140 ± 3	1.46
1.00	11 ± 3	72 ± 12	81 ± 6	10 ± 4	8 ± 1	109 ± 13	1.10
3.16	15 ± 4	82 ± 6	65 ± 9	11 ± 4	6 ± 1	118 ± 8	0.81
10.00	10 ± 3	56 ± 7	39 ± 3	8 ± 2	5 ± 1	33 ± 23	0.36
31.60	10 ± 6	45 ± 8	41 ± 2	10 ± 7	6 ± 2	32 ± 26	0.29
Positive control substances							
2-Aminoanthracene	2166 ± 808	2567 ± 1415	2133 ± 665	102 ± 19	17 ± 12	14 ± 6	0.13
Benzo[α]pyrene	1133 ± 153	1100 ± 153	1200 ± 173	18 ± 4	75 ± 44	189 ± 7	1.25

DOI: 10.1002/ptr

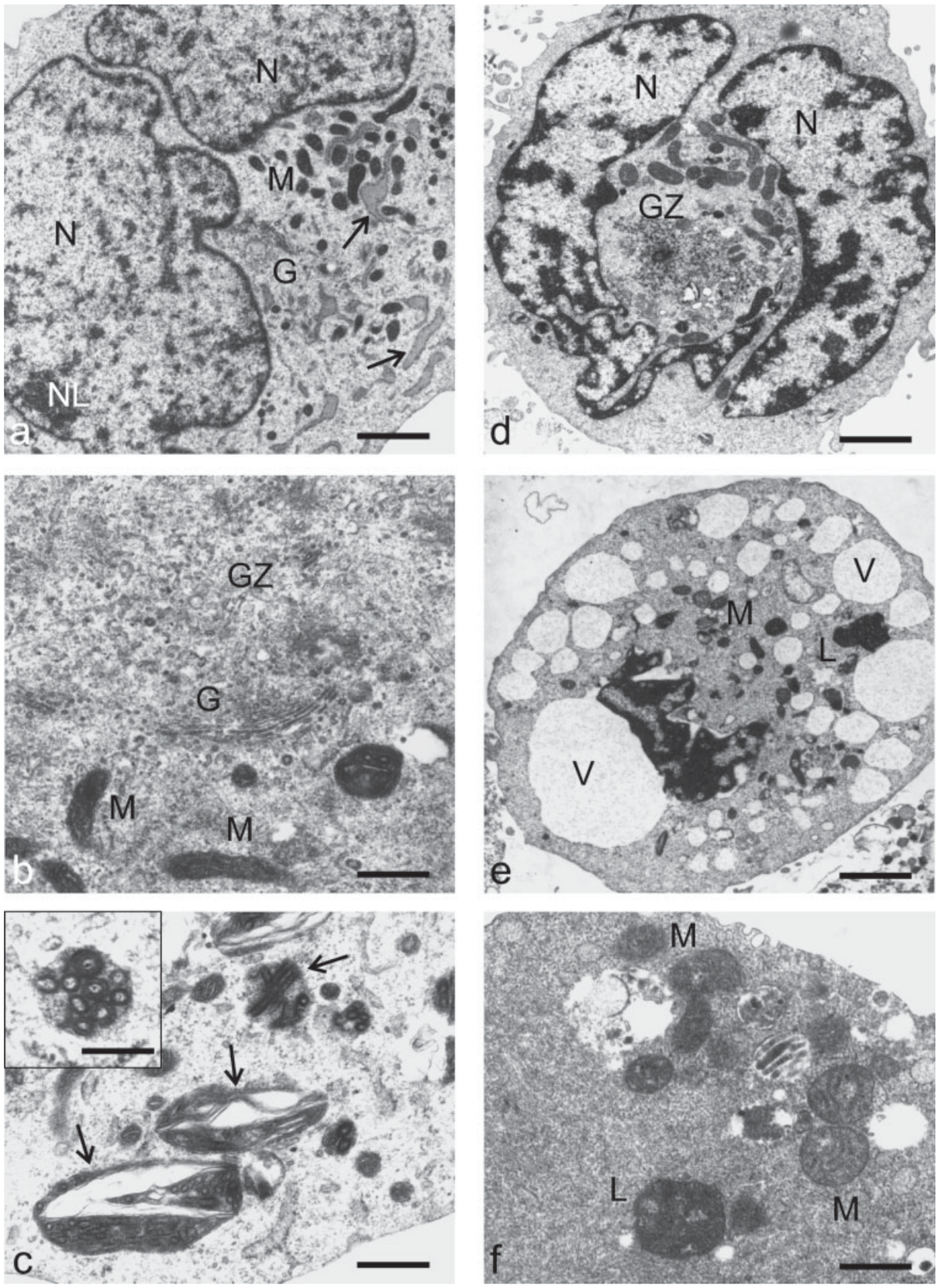

Figure 6. Electron micrographs. G1 cells: nontreated (a–c) and treated (d–f). (a) Normal cell with deeply lobed nucleus (N). Chromatin in small, loosely structured and randomly scattered flakes. The nucleolus (NL) is inconspicuous. Arrows point to dilated strands of RER. G, Golgi complex; M, mitochondria. Bar = 1.77 μm. (b) Normal cell. Golgi complex (G) surrounded by many small vesicles creating a Golgi zone (GZ); M, mitochondria. Bar = 0.65 μm. (c) Normal cell with complex tubular structures (arrows). Bar = 0.66 μm. (Inset) Bundle of tubules in cross section. Bar = 0.25 μm. (d) Treated cell (1 μL/mL). The nucleus (N) shows patches of condensed chromatin. The lobed nucleus embraces a Golgi zone (GZ) and mitochondria. Bar = 1.77 μm. (e) Treated cell (1 μL/mL) at progressed stage of cell death. The nucleus is pycnotic, the cytoplasm strongly vesiculated. The vesicles (V) contain a fine fibrous material. L, lysosomes; M, mitochondria. Bar = 1.85 μm. (f) Mitochondria (M) of treated cell (1 μL/mL) appear swollen. Cristae are less tightly packed, and the matrix is less electron-dense than in normal cells. L, lysosomes. Bar = 0.65 μm.

DOI: 10.1002/ptr

used as an early apoptosis marker. It binds to phospholipid phosphatidylserine when translocated from the inner to the outer leaflet of the plasma membrane – a first step in apoptosis. In none of the four carcinoma cell lines did the treatment with *I. helenium* extract enhance Annexin V-reactivity above reactivity of controls. At the same time, the vital dye propidium iodide stained 90% of the cells of all four cell lines after 24 h at 10-times the LD_{50}, indicating that the integrity of the plasma membrane was breached and necrosis was initiated.

Extensive electron microscope studies provided a detailed picture of the subcellular changes taking place. There was a remarkable correspondence of the effects observed in the four cell lines. Chromatin shows patchy, primarily marginal areas of condensation (Figs 3c, 4c, 6d), that were, at early stages, not as prominent as may be expected in apoptotic cells (Ress *et al.*, 2000). Shortly before cellular disintegration, chromatin condensation was more pronounced (Figs 4d, 6e). The nucleolus stayed intact until cytoplasmic degradation; nuclear fragmentation was not observed. Cytoplasmic vesiculation took place in all cell lines. First signs were a slight distension of the ER (including the nuclear envelope) and a lightening of its contents (Figs 3c, 4c, 5d). Then small irregular vesicles appeared which became very large, by fusion, and round before the cells ruptured (Figs 4d, 5e, 6e). Another common reaction to the extract: the mitochondria adopted pathological features. They appeared swollen, cristae became disorganized, and the matrix electron-lucent. In some cases, they seemed to break up and rupture (Figs 3d, 4e, f, 5f, 6f). The response time to treatment varied among the cells, which allowed a reconstruction of the time course of cellular breakdown.

All morphological changes point to necrotic cell death (Wyllie *et al.*, 1980). Lysosomal activity increased in some cells, but a pronounced autophagic activity was not discernible. It has been reported that intermediate and micro-filaments are largely preserved in autophagic PCD, but not in apoptosis (Bursch *et al.*, 2000). Some of the used cell lines include many intermediate filaments (Figs 3b, 5c). After treatment with the extract, bundles of the filaments appeared more electron-dense, probably caused by clumping (Fig. 5g) and tended to embrace cell organelles (Figs 3c, 4e). But this was not connected with autophagic processes, as is the case after treatment of MCF-7 cells with tamoxifen (Bursch *et al.*, 2000). However, it has become increasingly clear that necrotic morphology does not necessarily exclude a programming of the cell death (Schweichel and Merker, 1973; Clarke, 1990; Zakeri *et al.*, 1995). Thus, classical triggers of apoptosis may induce necrotic-like cell death characterized by cytoplasmic vacuolization and by minimal nuclear changes when caspase activities are inhibited. This implies that cells are equipped with two death programs: one that is caspase-dependent and shows apoptotic morphology, and another that is caspase-independent and shows necrotic-like morphology (see Kitanaka and Kuchino, 1999, for review). These authors take the view that caspase-independent PCD with necrotic-like morphology is not an exception but rather a common event. Interestingly, TNF (tumor necrosis factor) treatment may induce either apoptosis or caspase-independent necrotic-like cell death depending on the cell type (Schulze-Osthoff *et al.*, 1994; Vercammen *et al.*, 1998). McCourt *et al.* (2000) reported that in a tumor cell line (DHD/K12/TRb) taurolidine (a derivative of the amino acid taurine) promoted apoptosis at lower and necrosis at higher concentrations. Clearly, *in vitro* and *in vivo* systems strongly suggest that genetically regulated PCD with necrotic morphology exists and might be linked to the apoptotic pathway.

This bears consequences for the treatment of diseases caused by the failure to induce PCD when appropriate during normal developmental patterning or tissue homeostasis – as is the case in tumorous growth. In the past, chemical therapy of tumor cells was generally attempted via induction of apoptosis. Chemicals causing necrotic reactions to cancer cells were usually not considered useful for therapy because of an assumed lack of differentiation between cancerous and healthy cells. Given the existence of a PCD pathway with necrotic-like morphology, chemicals inducing this pathway could exert the same degree of specificity as do apoptosis-eliciting compounds. Moreover, they would be very beneficial in cases where cancerous cells have gained resistance to apoptosis (Kitanaka and Kuchino, 1999; Williams, 1991; Fisher, 1994). The extract of *I. helenium*, which causes a necrotic-like morphology in all four tested cancer cell lines, shows more than a hundred times lower toxicity against healthy human PBLs. It is expected that the extract activates a physiologically regulated suicidal program (with necrotic-like morphology) that is, for still unknown reasons, more easily accessible in cancerous than in healthy cells. The mode of action of the *I. helenium* extract and its potential for cancer therapy will be further analysed. Its lack of mutagenic activity is a further advantage for its eventual use in cancer treatment.

Acknowledgements

We thank Ms Elisabeth Sehn and Ms Margarethe Ullmann for excellent technical support.

REFERENCES

Ames BN, McCann J, Yamasaki E. 1975. Methods for detecting carcinogens and mutagens with the *Salmonella*/mammalian-microsome mutagenicity test. *Mutat Res* **31**: 347–364.

Bursch W, Ellinger A, Gerner C, Fröhwein U, Schulte-Hermann R. 2000. Programmed cell death (PCD): apoptosis, autophagic PCD, or others? *Ann NY Acad Sci* **926**: 1–12.

Bursch W, Hochegger K, Török L, Marian B, Ellinger A, Schulte-Hermann RS. 2000. Autophagic and apoptotic types of programmed cell death exhibit different fates of cytoskeletal filaments. *J Cell Sci* **113**: 1189–1198.

Cantrell CL, Abate L, Fronczek FR, Franzblau SG, Quijano L, Fischer NH. 1999. Antimycobacterial eudesmanolides from *Inula helenium* and *Rudbeckia subtomentosa*. *Planta Med* **65**: 351–355.

Clarke PGH. 1990. Developmental cell death: morphological diversity and multiple mechanisms. *Anat Embryol* **181**: 195–213.

Crown JC, O'Leary M, Ooi W-S. 2004. Docetaxel and paclitaxel in the treatment of breast cancer: a review of clinical experience. *Oncologist* **9** (suppl. 2): 24–32.

Dachler M, Pelzmann H. 1999. *Arznei- und Gewürzpflanzen* (2. Aufl.). Österreichischer Agrarverlag: Klosterneuburg (Austria).
Fisher DE. 1994. Apoptosis in cancer therapy: crossing the threshold. *Cell* **78**: 539–542.
Gligorov J, Lotz JP. 2004. Preclinical pharmacology of the taxanes: implications of the differences. *Oncologist* **9** (suppl. 2): 3–8.
Harvey RG, Goh SH, Cortez C. 1975. 'K-region' oxides and related oxidized metabolites of carcinogenic aromatic hydrocarbons. *J Am Chem Soc* **97**: 3468–3479.
Kitanaka C, Kuchino Y. 1999. Caspase-independent programmed cell death with necrotic morphology. *Cell Death Differ* **6**: 508–515.
Konishi Z, Shimada Y, Nagao T, Okabe H, Konoshima T. 2002. Antiproliferative sesquiterpene lactones from the roots of *Inula helenium*. *Biol Pharm Bull* **25**: 1370–1372.
List PH, Hörhammer L (eds). 1976. *Hagers Handbuch der pharmazeutischen Praxis, vierte Neuausgabe*, fünfter Band: *Chemikalien und Drogen*. Springer-Verlag: Berlin.
McCourt M, Wang JH, Sookhai S, Redmond HP. 2000. Taurolidine inhibits tumor cell growth *in vitro* and *in vivo*. *Ann Surg Oncol* **7**: 685–691.
Ortholand J-Y, Ganesan A. 2004. Natural products and combinatorial chemistry: back to the future. *Curr Op Chem Biol* **8**: 271–280.
Ress C, Holtmann M, Maas U, Sofsky J, Dorn A. 2000. 20-Hydroxyecdysone-induced differentiation and apoptosis in the *Drosophila* cell line, l(2)mbn. *Tissue Cell* **32**: 464–477.
Schulze-Osthoff K, Krammer PH, Droge W. 1994. Divergent signalling via APO-1/Fas and the TNF receptor, two homologous molecules involved in physiological cell death. *EMBO J* **13**: 4587–4596.
Schweichel JU, Merker HJ. 1973. The morphology of various types of cell death in prenatal tissues. *Teratology* **7**: 253–266.
Van Tellingen O, Sips JHM, Beijnen JH, Bult A, Nooijen WJ. 1992. Pharmacology, bio-analysis and pharmacokinetic derivatives. *Anticancer Res* **12**: 1699–1716.
Vercammen D, Beyaert R, Denecker G *et al.* 1998. Inhibition of caspases increases the sensitivity of L929 cells to necrosis mediated by tumor necrosis factor. *J Exp Med* **187**: 1477–1485.
Vickers A. 2002. Botanical medicines for the treatment of cancer: rationale, overview of current data, and methodological considerations for phase I and II trials. *Cancer Invest* **20**: 1069–1079.
Williams GT. 1991. Programmed cell death: apoptosis and oncogenesis. *Cell* **65**: 1097–1098.
Wyllie AH, Kerr JFR, Currie AR. 1980. Cell death: the significance of apoptosis. *Int Rev Cytol* **68**: 251–306.
Zakeri Z, Bursch W, Tenniswood M, Lockshin RA. 1995. Cell death: programmed, apoptosis, necrosis or other? *Cell Death Differ* **2**: 87–96.

DOI: 10.1002/ptr